



# The effect of $\text{CaF}_2$ and $\text{BaF}_2$ solid lubricants on wear resistance of laser-borided 100CrMnSi6-4 bearing steel

**A. Piasecki \*, M. Kotkowiak, M. Kulka**

Institute of Materials Science and Engineering, Poznan University of Technology,  
Pl. M. Skłodowskiej-Curie 5, 60-965 Poznań, Poland

\* Corresponding e-mail address: adam.piasecki@put.poznan.pl

## ABSTRACT

**Purpose:** In this paper, laser alloying with boron and solid lubricants was used in order to produce the self-lubricating layer on 100CrMnSi6-4 bearing steel. The influence of  $\text{CaF}_2$  and  $\text{BaF}_2$  on microstructure, hardness, chemical and phase composition as well as wear resistance of the layers was studied.

**Design/methodology/approach:** The two-step process was used during laser alloying. First, the surface of the specimen was coated by a paste with alloying material. The alloying material consisted of the mixture of amorphous boron and self-lubricating additions ( $\text{CaF}_2$  and  $\text{BaF}_2$ ). Next, the surface was re-melted by a laser beam using TRUMPF TLF 2600 Turbo  $\text{CO}_2$  laser. The laser beam power 1.43 kW was used for laser alloying. The layer was characterized using X-ray diffraction, Scanning Electron Microscopy, Energy Dispersive Spectroscopy, microhardness tester. The dry sliding wear behaviour of the layer was investigated using the Amsler type wear test.

**Findings:** The tribofilm, consisting of solid lubricants, was observed on the worn surfaces of laser-alloyed layers. It caused an increase in the wear resistance at room temperature. The presence of calcium fluoride and barium fluoride was confirmed in laser-alloyed layers using XRD and X-ray microanalysis by EDS method.

**Practical implications:** Laser surface modification with solid lubricants had the important cognitive significance and gives grounds to the practical employment of this technology for reducing the abrasive wear.

**Originality/value:** The wear mechanism of surface layer with solid lubricants was determined. The produced layer with laser alloying layers of boron and solid lubricant ( $\text{CaF}_2$  or  $\text{BaF}_2$ ) was compared.

**Keywords:** Laser boriding; Self-lubricating additions; Microstructure; Hardness; Wear resistance

**Reference to this paper should be given in the following way:**

A. Piasecki, M. Kotkowiak, M. Kulka, The effect of  $\text{CaF}_2$  and  $\text{BaF}_2$  solid lubricants on wear resistance of laser-borided 100CrMnSi6-4 bearing steel, Archives of Materials Science and Engineering 86/1 (2017) 15-23.

## PROPERTIES

## 1. Introduction

The wear of machinery and tools because of friction caused a lot of financial loss related to the replacement of these parts. Surface engineering provided the methods which could counteract the friction. Carburizing [1], nitriding [2-5], boriding and borochromizing [6,7], CVD [8] or PVD [8-10] methods, galvanic methods as well as laser surface treatment [11,12] belonged to such a surface treatment. The wear resistance of materials was very often improved by increasing the hardness because the surface layer with higher hardness was characterized by the better tribological properties. The present study showed that the surface layers could be characterized by higher wear resistance despite the lower microhardness. The improvement of wear resistance was obtained by the addition of solid lubricants (calcium and barium fluorides) to the layers during the laser alloying process. Nowadays, the new solid lubricants were often used in nanometric scale [13,14]. The friction coefficients, characteristic of friction pair, could also be reduced by oils. However, oils were very dangerous in the use, during production and utilization. Therefore, the importance of solid lubricants increased. Solid lubricants could be divided into: metals, fluorides, sulfides, sulfur and tungstates [15,16]. Molybdenum disulfide  $\text{MoS}_2$  was very popular, but it couldn't work at elevated temperatures [17,18]. Fluorides  $\text{CaF}_2$  and  $\text{BaF}_2$  became very important because of their possible use at elevated temperatures, resulting in the reduction of friction coefficient. During the wear tests, the tribofilm, based on solid lubricants, was produced on the worn surface and protected the mating parts against wear. This phenomenon was previously observed between friction pair consisting of self-lubricating surface layer and sintered carbide S20S [19,20]. In this work, the influence of laser alloying with B,  $\text{CaF}_2$  and  $\text{BaF}_2$  on the microstructure and properties of 100CrMnSi6-4 bearing steel was studied.

## 2. Experimental procedure

### 2.1. Material

In Table 1, the chemical composition of investigated 100CrMnSi6-4 bearing steel was shown. The ring-shaped specimens had external diameter equal to 20 mm, internal diameter – 12 mm and height – 12 mm.

Table 1.

Chemical composition of 100CrMnSi6-4 bearing steel, wt.%

C	Cr	Mn	Si	Cu	P	S	Fe
1.03	1.52	1.08	0.59	0.11	0.022	0.012	bal.

### 2.2. Laser alloying

The laser boriding with the addition of solid lubricant material was conducted as the two step process (Fig. 1). At first, the outer surface of the sample was coated by the paste, which was made from amorphous boron, barium fluoride ( $\text{BaF}_2$ ) and calcium fluoride ( $\text{CaF}_2$ ) powders with the mass ratio of 10:1:1. The thickness of the paste was equal to 60  $\mu\text{m}$  and 100  $\mu\text{m}$ . During the next step, the surface with the paste was irradiated by the laser beam. The TRUMPF TLF 2600 Turbo  $\text{CO}_2$  laser, with the nominal power equal to 2.6 kW, was used in this investigation. During the laser alloying, laser beam power  $P=1.43$  kW was used. The thickness of the paste coating was 100  $\mu\text{m}$ . The other parameters of the laser treatment were as follows: laser beam diameter  $d=2$  mm and scanning rate  $v_f=2.88$  m/min.

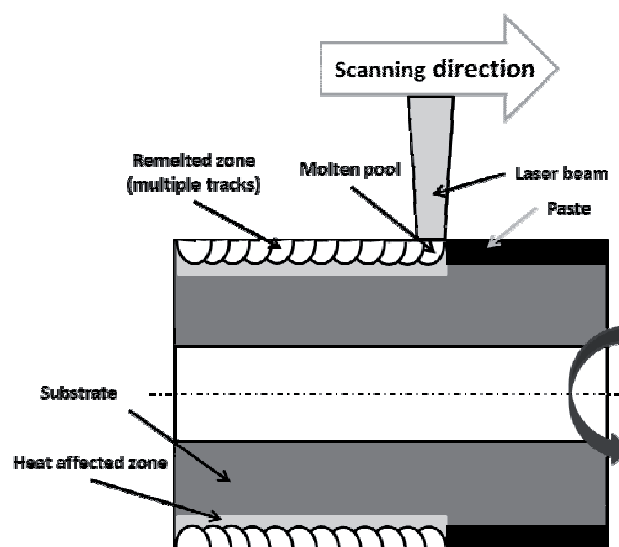


Fig. 1. Scheme of two-step method of laser-alloying

### 2.3. Microstructure and microhardness

The polished and etched cross sections were used for the microstructural observations. The samples were polished,

at first, by the abrasive papers, which were characterized by the different granularity and after that with Al<sub>2</sub>O<sub>3</sub>. The samples were etched by the reagent consisting of 5% nital. Optical microscope (OM) and scanning electron microscope (SEM) Tescan Vega 5135 were used for microstructure observation. The PANalytical EMPYREAN diffractometer with Cu K<sub>α</sub> radiation was applied for phase analysis. Microhardness profiles were performed by the Buehler Micromet II apparatus, with a load equal to 50 gf (approximately 0.49 N).

#### 2.4. Wear test

Wear resistance tests were carried out under dry friction conditions with the use of MBT-01 device. The frictional pair, which was shown in Fig. 2, consisted of ring-shaped sample and S20S sintered carbide as a counter-sample. In the Table 2, the chemical composition of counter specimen was shown. The sintered carbide S20S density was equal to 10.7 g/cm<sup>3</sup> and hardness – 1430 HV. The parameters of the wear test were as follows: load  $F=49$  N, and a specimen speed 0.26 m/s, resulting from the tangential speed of the specimen surface and rotational speed  $n=250$  min<sup>-1</sup>. The results of wear test were analyzed by relative loss of mass of the specimen and counter-specimen. The worn surfaces after wear test were analyzed by the scanning electron microscope (SEM) equipped with an energy dispersive spectrometer (EDS) PGT Avalon.

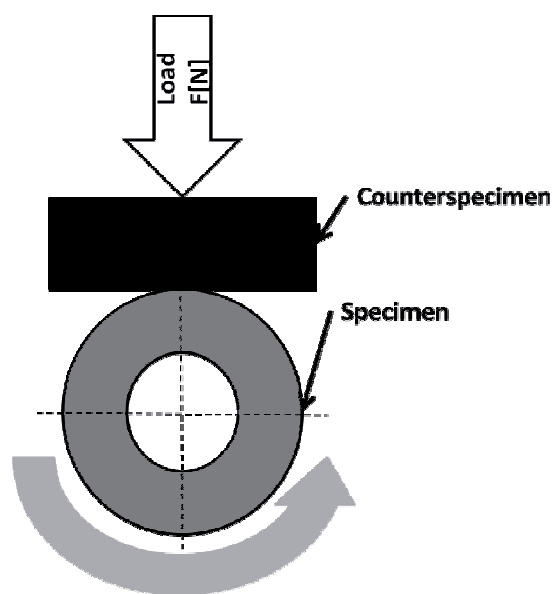


Fig. 2. Scheme of the wear test

Table 2.

Chemical composition of sintered-carbide S20S, wt.%

WC	TiC+TaC+NbC	Co
58	31.5	10.5

$$\frac{\Delta m}{m_i} = \frac{m_i - m_f}{m_i} \quad (1)$$

where:  $\Delta m$  is a loss of mass [mg],  $m_i$  is an initial mass of the specimen or counter-specimen [mg],  $m_f$  is a final mass of the specimen or counter-specimen [mg].

### 3. Results

The XRD results were shown in Fig. 3. Based on these studies, the produced layer consisted of a mixture of borides (FeB, Fe<sub>2</sub>B, Fe<sub>3</sub>B), borocementite Fe<sub>3</sub>(B,C) and martensite (identified as Fe- $\alpha$ ). The presence of barium and calcium fluorides as separate phases was also confirmed. The phase analysis was performed immediately after laser alloying on the treated surface using Cu K<sub>α</sub> radiation. The use of this radiation usually enabled to analyze the depth up to 20  $\mu$ m, i.e. in re-melted zone.

The microstructure of laser-borided layer obtained on 100CrMnSi6-4 with CaF<sub>2</sub> and BaF<sub>2</sub> solid lubricants was shown in Figs. 4-6. Analysis using OM (Fig. 4) showed that the three zones were observed in an areological system: laser-remelted zone MZ (1), heat-affected zone – HAZ (2) and substrate without visible effects of heat treatment (3). The obtained layer was continuous, compact and uniform in respect of its thickness. It was related to a high overlapping of the multiple laser tracks (86%). The average thickness of the laser-remelted zone was equal to about 400  $\mu$ m, whereas the average thickness of heat-affected zone was about 190  $\mu$ m.

In microstructure of MZ, the phases, identified by XRD (see Fig. 3), were observed. Microstructure of the heat-affected zone, directly below the remelted layer (marked as 2a), was characterized by the presence of martensite and retained austenite. The microstructure of the region, marked as 2b, probably consisted of sorbite and pearlite.

Similar microstructures of the heat affected zones were obtained for the samples examined in the previous study [19,20]. So, the changeable microstructure of HAZ resulted from the different conditions of the laser treatment at different depths of laser heat-treated steel with a paste consisting of boron and solid lubricants.

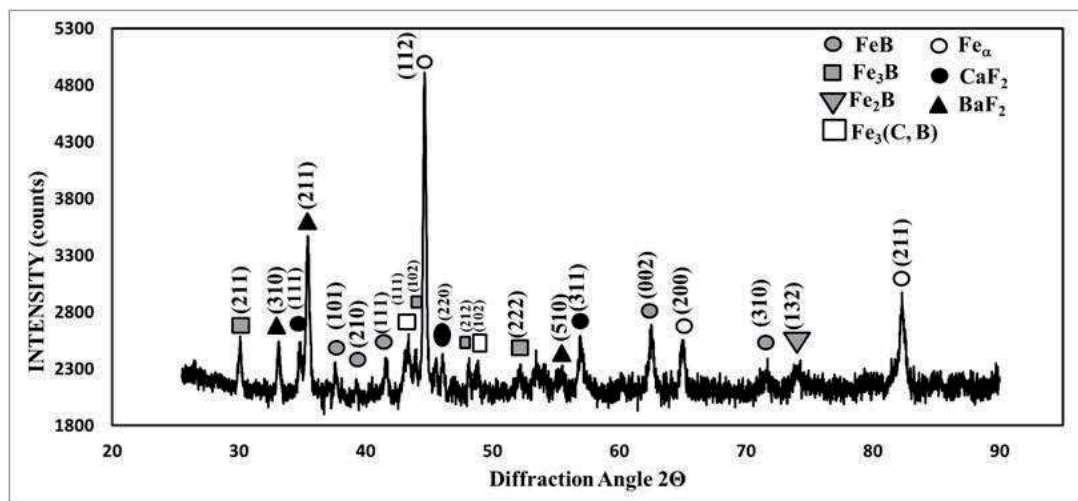


Fig. 3. XRD pattern of laser-alloyed 100CrMnSi6-4 steel with boron,  $\text{CaF}_2$  and  $\text{BaF}_2$

The presence of sorbite could result from the high-temperature tempering of this region during the formation of adjacent tracks. The presence of martensite and retained austenite, directly below MZ, was a consequence of the high carbon content and higher cooling rate in this zone compared to the areas, locating at higher depth.

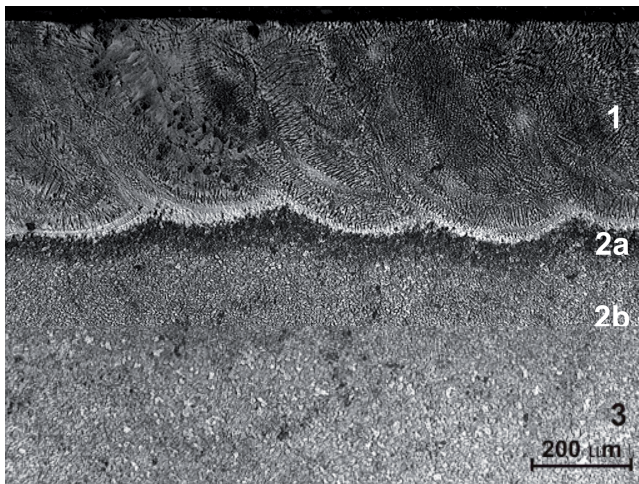


Fig. 4. OM microstructure of laser-alloyed 100CrMnSi6-4 steel with boron,  $\text{CaF}_2$  and  $\text{BaF}_2$ ; 1 – remelted zone (MZ), 2 – heat-affected zone (HAZ), 3 – substrate; OM

The detailed analysis of the microstructure of the laser-alloyed layer was carried out using SEM (Fig. 5). The light particles of solid lubricants were clearly visible, mainly close to the surface, up to the depth of about 50-60  $\mu\text{m}$ . The particles of  $\text{CaF}_2$  and  $\text{BaF}_2$  were located in the eutectic

mixture between the borides. Such a distribution of solid lubricants was advisable taking into consideration wear behavior of the alloyed layer. It facilitated delivering solid lubricants into the contact area of mating parts and the formation of tribofilm between them. The MZ consisted of dendritic or globular iron borides as well as of eutectic mixture of borides, borocementite and martensite, according to the results of XRD.

The presence of particles of solid lubricants, close to surface, could be explained, taking into account their low density. During the re-melting process, these phases, having low density compared to the density of the molten pool, came up to the surface and some of the particles due to convection motions were trapped deeper.

The relatively small amount of fluorides in metallographic specimens resulted from their preparation. During preparing the metallographic specimen, some of solid lubricant particles could be rinsed out. These fluorides ( $\text{CaF}_2$  and  $\text{BaF}_2$ ) should be applied as lubricants working in dry conditions, i.e. in the environment free from water and even damp. The microstructure analysis by OM, SEM and XRD confirmed that the parameters of the laser alloying process were properly selected and avoid substantial thermal decomposition and vaporization of calcium and barium fluoride.

The method of hardness measurements, i.e. hardness indents in the OM image of the laser alloyed layer, were shown in Fig. 6. Whereas the microhardness profiles in the laser-alloyed layer were presented in Fig. 7. Measurements were performed at right angles to the surface along the axis of laser track, at the contact of tracks (Fig. 7a) as well as

horizontally along the layer at a distance from the surface of 50  $\mu\text{m}$  and at the boundary between the remelted zone and the heat affected zone (Fig. 7b).

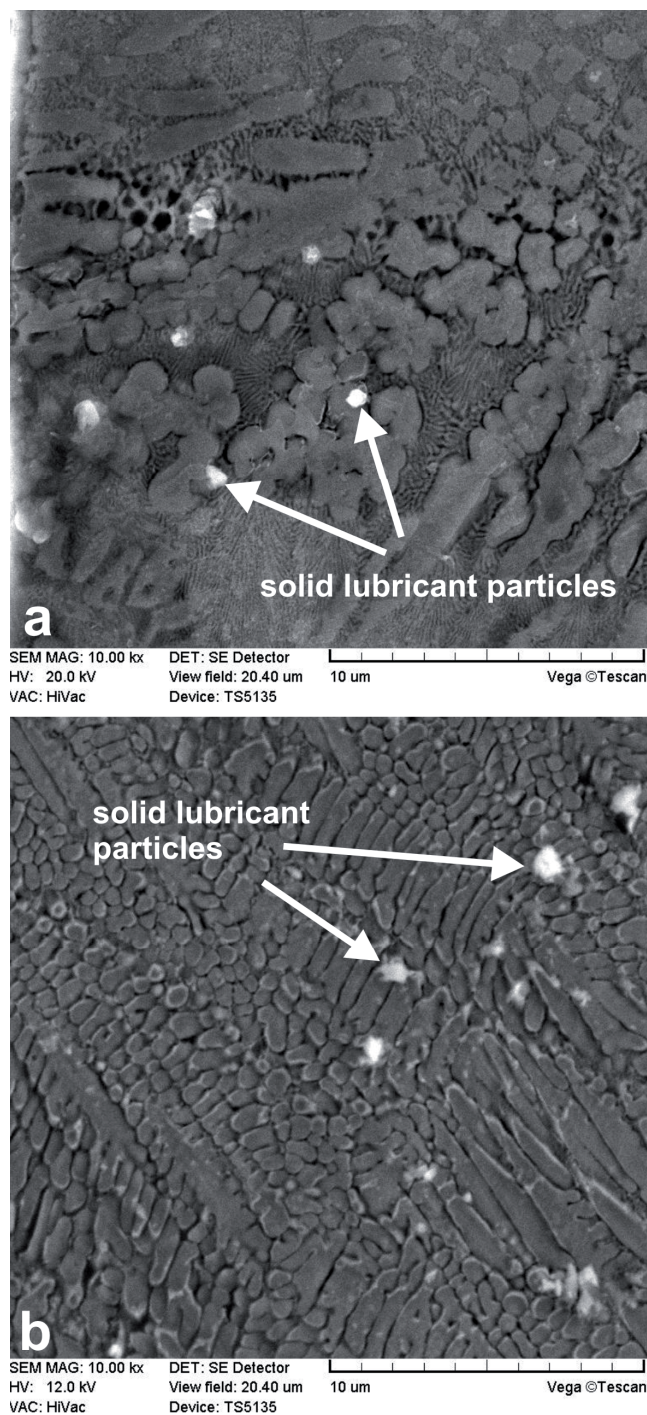


Fig. 5. SE images of laser-allyed 100CrMnSi6-4 steel with boron,  $\text{CaF}_2$  and  $\text{BaF}_2$ ; SEM

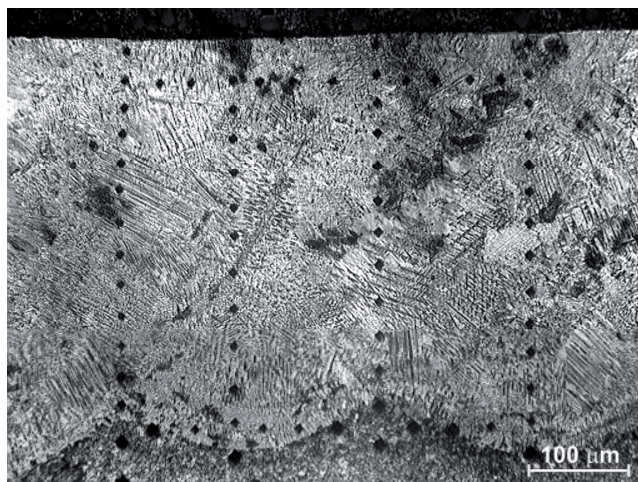


Fig. 6. Hardness indentations in OM microstructure of laser-allyed 100CrMnSi6-4 steel with boron,  $\text{CaF}_2$  and  $\text{BaF}_2$

For the obtained layer, microhardness of MZ varied between 665 and 810 HV in the axis of a laser track and between 613 and 795 HV at the contact of tracks. The microhardness of the re-melted zone at the distance 50  $\mu\text{m}$  from the surface was between 608 and 810 HV. There were no differences in hardness, relating to the place of measurements, i.e. the similar hardness was characteristic of the axis of a laser track and of the contact of tracks. The previous work [19] reported that the hardness of the laser-allyed layer with boron only, was characterized by higher hardness of MZ (in the range of 875-1450HV). In the present study, the laser-allyed layer was characterized by the similar hardness to that-reported by the papers [19,20], concerning the laser-allyed layers with boron and  $\text{CaF}_2$  or with boron and  $\text{BaF}_2$ . The hardness of HAZ ranged from 241 to 437 HV. During the transition of the first laser beam and rapid cooling in the heat affected zone, martensite and retained austenite were formed. During the transition of consecutive laser beam tracks, the previous track was tempered. The higher the tempering temperature, resulting from the laser beam power, the lesser the hardness of zones of the treated material. Differences in hardness in the cross-section of the layer were due to the multi-phase microstructure, consisting of martensitic, eutectic, and hard boride phases detected in the XRD studies.

Wear tests at the load of 49 N under dry friction conditions were performed. Wear resistance was studied for 2 h, with a change in the counter-specimen every 0.5 h.

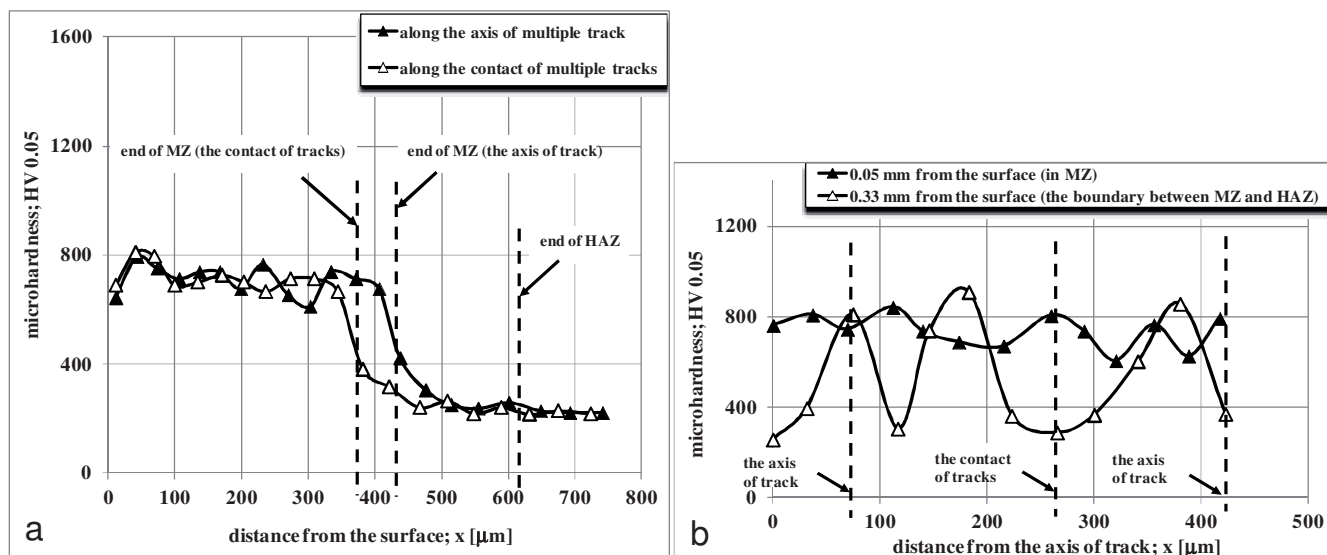


Fig.7. Microhardness profiles of laser-alloyed 100CrMnSi6-4 steel with boron, CaF<sub>2</sub> and BaF<sub>2</sub>

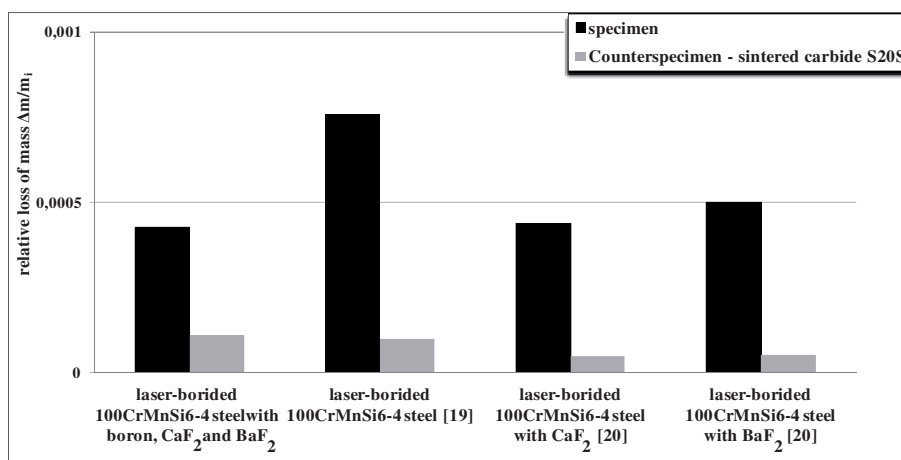


Fig. 8. Results of wear tests; relative mass loss of specimens and counter-specimens after two-hour wear test with the change of counter-specimen every 0.5 hour (load F=49 N)

The results were shown in Figs. 8-10 and compared to those-obtained during the previous studies [19,20]. Based on all the tests, it could be reported that laser-borided layers modified by the addition of CaF<sub>2</sub> and/or BaF<sub>2</sub> were characterized by higher resistance to friction in dry conditions compared to the laser-alloyed layer with boron only. In spite of the diminished hardness of laser-alloyed layers with solid lubricants, the wear of these layers were smaller than that-characteristic of the typical laser-borided layer (Fig. 8).

Decreased wear, measured by relative mass loss of specimen and counter-specimen, was observed due to the formation of the tribofilm between the mating pair that protected both surfaces. The presence of the tribofilm, composed of the used in this work solid lubricants (CaF<sub>2</sub> and BaF<sub>2</sub>), on the worn surface of laser-alloyed layer was reported by the X-ray microanalysis (Fig. 9) and SEM observations (Fig. 10). The increased concentration of barium and calcium was clearly visible in the EDS surface distribution of elements (Figs. 9b and c).

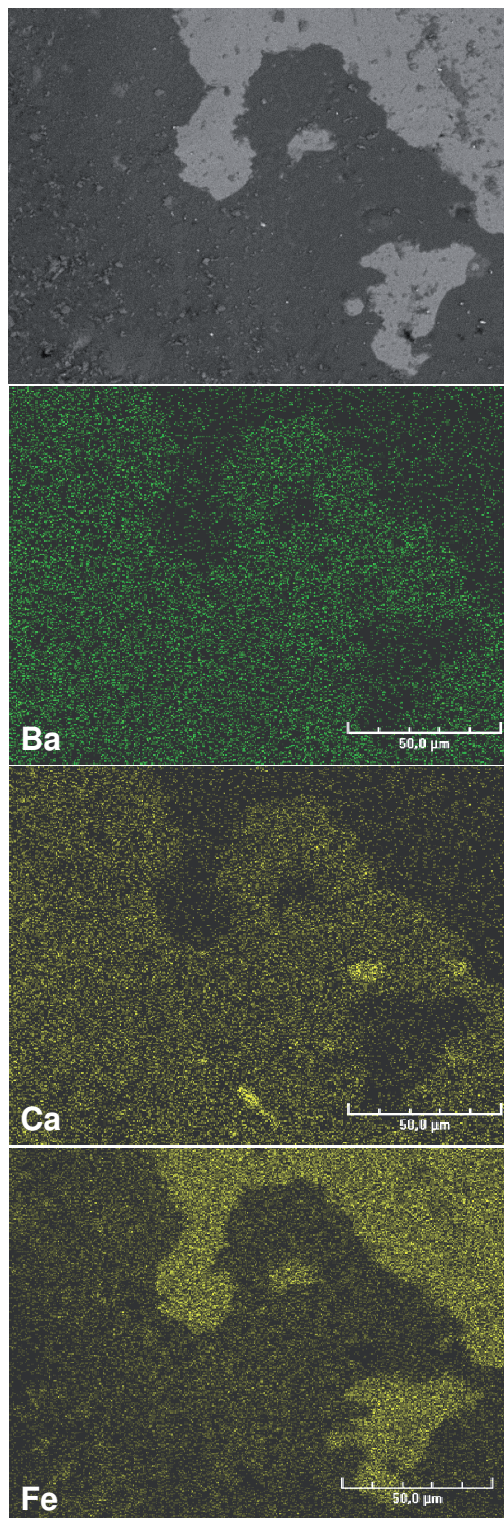


Fig. 9. Worn surface of laser-alloyed 100CrMnSi6-4 steel with boron,  $\text{CaF}_2$  and  $\text{BaF}_2$ . EDS patterns of barium, calcium and iron

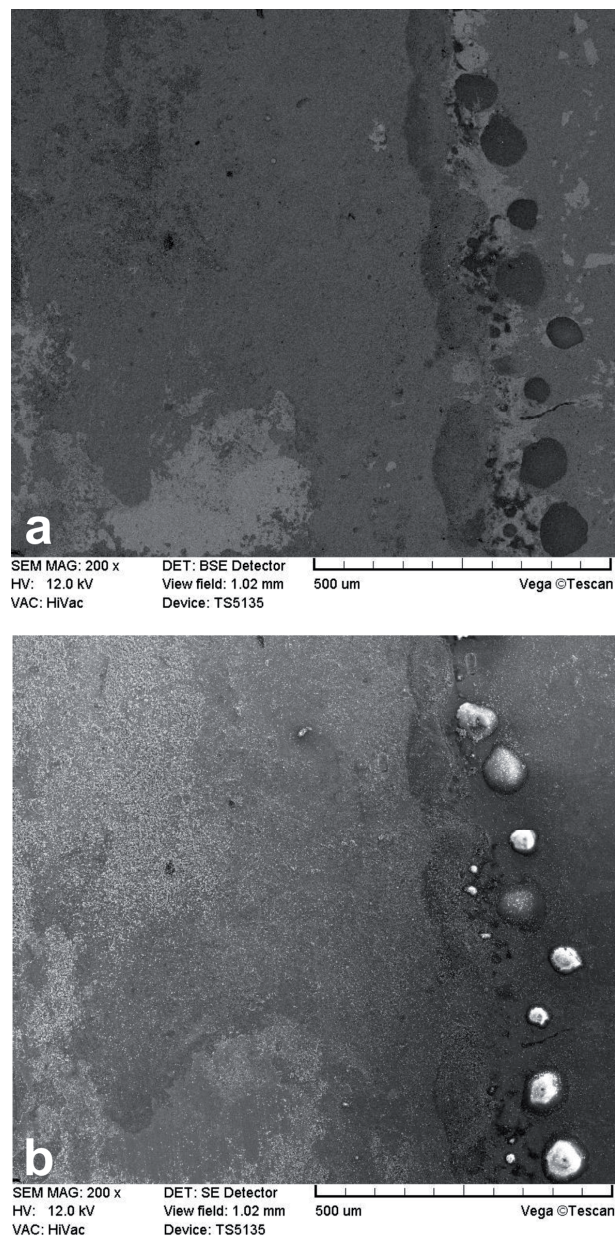


Fig. 10. Worn surface of laser-alloyed 100CrMnSi6-4 steel with boron,  $\text{CaF}_2$  and  $\text{BaF}_2$

In Figure 10, the worn surface in BSE and SE contrasts was shown. The tribofilm was clearly visible in that case, especially, in BSE image (Fig. 10a). Darker areas were characterized by the presence of light elements, such as Ca, Ba and F. The diversified grayscale could attest to the different thickness of the tribofilm. Brighter areas corresponded to the tribofilm of smaller thickness. To reduce the depth of the of electron interaction, the test at an accelerating voltage of 12 kV was used. Based on BSE

image and EDS spectroscopy, the presence of the tribofilm with solid lubricants of different thickness was confirmed. The schemes of tribofilm producing were presented in the previous studies [19,20]. The formation of tribofilm consisted of the three stages: lapping, smearing lubricants on the worn surface and, appearance of the tribofilm of diversified thickness.

#### 4. Conclusions

Laser-boriding with the addition of calcium fluoride ( $\text{CaF}_2$ ) and barium fluoride ( $\text{BaF}_2$ ) was applied to produce self-lubricating surface layer on 100CrMnSi6-4 bearing steel. Because of high overlapping of multiple laser tracks (86%), the continuous, compact and uniform in respect of its thickness laser-alloyed layer was produced. The microstructure was characterized by the three zones: laser re-melted zone, heat-affected zone and the substrate without visible changes in microstructure. The re-melted zone consisted of eutectic mixture of iron borides, borocementite and martensite as well as of the particles of solid lubricants. They were visible mainly close to the surface, up to the depth of about 50-60  $\mu\text{m}$ . The obtained layer had an average thickness of about 400  $\mu\text{m}$  and hardness at the surface equal to 800 HV. Hardness and wear resistance of the produced layer was similar to the laser-borided layers with the addition of only  $\text{CaF}_2$  or only  $\text{BaF}_2$ . The significant increase in wear resistance of laser-borided layer with  $\text{CaF}_2$  and  $\text{BaF}_2$  was observed, particularly, in comparison with the laser-alloyed layer with boron only. However, the produced layers could be classified regarding the wear resistance as follows: the highest wear resistance was characteristic of the laser-borided layer with  $\text{CaF}_2$  addition only, next, the laser-borided layer with  $\text{CaF}_2 + \text{BaF}_2$  mixture and, finally, the laser-borided layer with  $\text{BaF}_2$  only. The increase in wear resistance was due to the formation of a tribofilm between the mating pair that protected counter and counter-specimen surfaces. The presence of the tribofilm, consisting of the used solid lubricant, was confirmed on the worn surface using XRD and X-ray microanalysis by EDS method.

#### Acknowledgements

This work has been financially supported by Ministry of Science and Higher Education in Poland as a part of the 02/24/DSPB Project.

#### References

- [1] M. Kulka, M. Przylecka, W. Gestwa, M. Piwecki, Influence of carburizing and heat treatment on the mechanical properties of LH15 grade bearing steel, *Materials Science Forum* 163-166/1 (1994) 215-220.
- [2] S. Taktak, I. Gunes, Effect of pulse plasma nitriding on tribological properties of AISI 52100 and 440C steels, *International Journal of Surface Science and Engineering* 8/1 (2014) 39-56.
- [3] X. Li, W. Yue, C. Wang, X. Gao, S. Wang, J. Liu, Comparing tribological behaviors of plasma nitride and untreated bearing steel under lubrication with phosphor and sulfur-free organotungsten additive, *Tribology International* 51 (2012) 47-53.
- [4] S. Wang, W. Yue, Z. Fu, C. Wang, X. Li, J. Liu, Study on the tribological properties of plasma nitrided bearing steel under lubrication with borate ester additive, *Tribology International* 66 (2013) 259-264.
- [5] W. Yue, Z. Fu, S. Wang, X. Gao, H. Huang, J. Liu, Tribological synergistic effects between plasma nitride 52100 steel and molybdenum dithiocarbamates additive in boundary lubrication regime, *Tribology International* 74 (2014) 72-78.
- [6] I. Ozbek, Mechanical properties and kinetics of borided AISI M50 bearing steel, *Arabian Journal for Science and Engineering* 39/6 (2014) 5185-5192.
- [7] S. Sen, U. Sen, The effect of boronizing and borochromizing on tribological performance of AISI 52100 bearing steels, *Industrial Lubrication and Tribology* 61/3 (2009) 146-153.
- [8] M. Nilsson, M. Olsson, Tribological testing of some potential PVD and CVD coatings for steel wire drawing dies, *Wear* 273 (2011) 55-59.
- [9] B. Podgornik, J. Vižintin, U. Borovšak, F. Megušar, Tribological properties of DLC coatings in helium, *Tribology Letters* 47/2 (2012) 223-230.
- [10] I.L. Rasmussen, M. Guibert, M. Belin, J.M. Martin, N.J. Mikkelsen, H.C. Pedersen, J. Schou, Wear monitoring of protective nitride coatings using image processing, *Surface and Coatings Technology* 204 (2010) 1970-1972.
- [11] E. Jonda, K. Labisz, L.A. Dobrzański, Microstructure and properties of the hot work tool steel gradient surface layer obtained using laser alloying with tungsten carbide ceramic powder, *Archives of Materials Science and Engineering* 78/1 (2016) 37-44.

- [12] M. Bonek, Formation of gradient surface layers on high speed steel by laser surface alloying process, *Archives of Materials Science and Engineering* 58/2 (2012) 182-192.
- [13] R. Harichandran, N. Selvakumar, Effect of h-BN solid nano lubricant on the dry sliding wear behaviour of Al-B<sub>4</sub>C nanocomposites, *Archives of Materials Science and Engineering* 77/1 (2016) 5-11.
- [14] J. Cho, Y. Xiong, J. Kim, C. Lee, S.Y. Hwang, Tribological behavior of NiCr-base blended and nanostructured composite APS coatings by rig test, *Wear* 265 (2008) 1565-1571.
- [15] J.F. Yang, Y. Jiang, J. Hardell, B. Prakash, Q.F. Fang, Influence of service temperature on tribological characteristics of self-lubricant coatings: a review, *Frontiers of Materials Science* 7/1 (2013) 28-39.
- [16] I.M. Allam, Solid lubricants for applications at elevated temperatures: A review, *Journal of Materials Science* 26/15 (1991) 3977-3984.
- [17] L. Kong, S. Zhu, Q. Bi, Z. Qiao, J. Yang, W. Liu, Friction and wear behavior of self-lubricating ZrO<sub>2</sub>(Y<sub>2</sub>O<sub>3</sub>)–CaF<sub>2</sub>–Mo–graphite composite from 20°C to 1000°C, *Ceramics International* 40 (2014) 10787-10792.
- [18] X. Zhang, L. Zhang, Z. Huang, Characterization of Ni-based alloy submicron WS<sub>2</sub>/CaF<sub>2</sub> composite coatings deposited by high velocity oxy-fuel (HVOF) spray process, *Advanced Materials Research* 881-883 (2014) 1407-1411.
- [19] A. Piasecki, M. Kulka, M. Kotkowiak, Wear resistance improvement of 100CrMnSi6-4 bearing steel by laser boriding using CaF<sub>2</sub> self-lubricating addition, *Tribology International* 97 (2016) 173-191.
- [20] A. Piasecki, M. Kotkowiak, M. Kulka, Self-lubricating surface layers produced using laser alloying of bearing steel, *Wear Part B* 376-377 (2017) 993-1008.